Size-Dependent Optical Spectroscopy of a Homologous Series of CdSe Cluster Molecules

V. N. Soloviev,[†] A. Eichhöfer,[‡] D. Fenske,[‡,§] and U. Banin*[,†]

Contribution from the Department of Physical Chemistry and the Farkas Center for Light Induced Processes, The Hebrew University, Givat Ram, Jerusalem 91904, Israel, the Institut für Nanotechnologie, Forschungszentrum Karlsruhe, Postfach 3640, 76021 Karlsruhe, Germany, and the Institut für Anorganische Chemie, Universität Karlsruhe, Engesserstrasse Geb. 30.45, D-76128 Karlsruhe, Germany

Received October 5, 2000

Abstract: The optical properties and electronic structure of a homologous series of CdSe cluster molecules covering a size range between 0.7 and 2 nm are investigated. CdSe cluster molecules with 4, 8 10, 17, and 32 Cd atoms, capped by selenophenol ligands, were crystallized from solution and their structures determined by single-crystal X-ray diffraction. The cluster molecules are composed of a combination of adamanthane and barylene-like cages, the building blocks of the zinc blende and the wurtzite structures of the bulk CdSe. The onset of the room temperature absorption and low-temperature photoluminescence excitation spectra exhibit a systematic blue shift with reduced cluster size manifesting the quantum confinement effect down to the molecular limit of the bulk semiconductor. Blue-green emission, shifted substantially to lower energy from the absorption onset, is observed only at low temperature and its position is nearly independent of cluster size. The wavelength dependence of both photoluminescence and photoluminescence excitation was measured. The emission is assigned to forbidden transitions involving the cluster-molecule surface-capping ligands. This assignment is supported by the emission decay which exhibits distributed kinetics with microsecond time scale. The temperature dependence of the emission intensity is quantitatively explained by multiphonon-induced nonradiative relaxation mediated by low-frequency vibrations of the selenophenol capping ligands. Upon irradiation, the emission of all cluster molecules is quenched. Warming up and recooling leads to recovery of the emission (partial or complete) for all but the cluster molecule with 10 Cd atoms. This temporary darkening is assigned to the photoinduced charging of the cluster-molecule surface ligands, resembling the reversible on−off blinking of the emission observed for larger CdSe nanocrystals.

Cluster molecules of semiconductor materials, composed of tens of atoms with bonding resembling that present in the solid state, are interesting molecular models for the bulk.[1,2] Their typical size range is below 2 nm, where only several closed-shell structures are stable, thus marking the transition from nanocrystals into cluster molecules with a well-defined chemical formula. Size-dependent electronic and optical properties manifesting quantum confinement effects have been studied extensively for larger nanocrystals, spanning the size range of 2 to 10 nm, using optical and tunneling spectroscopy as well as theoretical analysis.[7−13] But only limited studies have been carried out on the electronic properties of semiconductor cluster molecules.[2,3,6] Recent progress in the synthesis of CdSe cluster molecules has led to a development of a homologous series of such compounds (Figure 1),[14−16] and the largest cluster molecule already overlaps in size with the smallest nanocrystals of this prototypical quantum dot system.[17,18] In a recent paper we reported on the observation of the blue shift of the absorption band gap in the cluster molecules with reduced size.[4] Thus, they also manifest the quantum confinement effect, continuing the dependence observed for larger CdSe nanocrystals.[17,18] Here we

* To whom correspondence should be addressed. E-mail: banin@chem.ch.huji.ac.il.

[†] The Hebrew University.

[‡] Forschungszentrum Karlsruhe.

[§] Universität Karlsruhe.

(1) Dance, I. G.; Choy, A.; Scudder, M. L. *J. Am. Chem. Soc.* **1984**, *106*, 6285.

(2) Herron, N.; Calabrese, J. C.; Farneth, W. E.; Wang, Y. *Science* **1993**, *259*, 1426.

(3) Vossmeyer, T.; Reck, G.; Katsikas, L.; Haupt, E. T. K.; Schulz, B.; Weller, H. *Science* **1995**, *267*, 1476.

(4) Soloviev, V.; Eichofer, A.; Fenske, D.; Banin, U. *J. Am. Chem. Soc.* **2000**, *122*, 2673.

(5) Türk, T.; Resch, U.; Fox, A. M.; Vogler, A. *J. Phys. Chem.* **1992**, *96*, 3818.

(6) Liu, H. J.; Hupp, J. T.; Ratner, M. A. *J. Phys. Chem.* **1996**, *100*, 12204.

(7) Alivisatos, A. P. *Science* **1996**, *271*, 933.

(8) Nirmal, M.; Brus, L. *Acc. Chem. Res.* **1999**, *32*, 407.

(9) Norris, D. J.; Sacra, A.; Murray, C. B.; Bawendi, M. G. *Phys. Rev. Lett.* **1994**, *72*, 2612. Norris, D. J.; Bawendi, M. G. *Phys. Rev. B* **1996**, *53*, 16338.

(10) Banin, U.; Cao, Y. W.; Katz, D.; Millo, O. *Nature* **1999**, *400*, 542.

(11) Ekimov, A. I.; Hache, F.; Schanne-Klein, M. C.; Ricard, D.; Flytzanis, C.; Kudryavtsev, I. A.; Yazeva, T. V.; Rodina, A. V.; Efros, A. L. *J. Opt. Soc. Am. B* **1993**, *10*, 100.

(12) Fu, H.; Zunger, A. *Phys. Rev. B* **1998**, *57*, R15064.

(13) Rabani, E.; Hetenyi B.; Berne, B. J.; Brus, L. E. *J. Chem. Phys.* **1999**, *110*, 5355.

(14) Behrens, S.; Bettenhausen, M.; Deveson, A. C.; Eichhöfer, A.; Fenske, D.; Lohde, A.; Woggon, U. *Angew. Chem., Int. Ed. Engl.* **1996**, *35*, 2215.

(15) Behrens, S.; Bettenhausen, M.; Eichhöfer, A.; Fenske, D. *Angew. Chem., Int. Ed. Engl.* **1997**, *24*, 2792.

(16) Behrens, S.; Fenske, D. *Ber. Bunsen-Ges. Phys. Chem.* **1997**, *101*, 1588.

(17) Murray, C. B.; Norris, D. J.; Bawendi, M. G. *J. Am. Chem. Soc.* **1993**, *115*, 8706.

(18) Rogach, A. L.; Koronowski, A.; Gao, M.; Eychmüler, A.; Weller H. *J. Phys. Chem. B* **1999**, *103*, 3065.

10.1021/ja003598j CCC: $20.00
Published on Web 02/16/2001

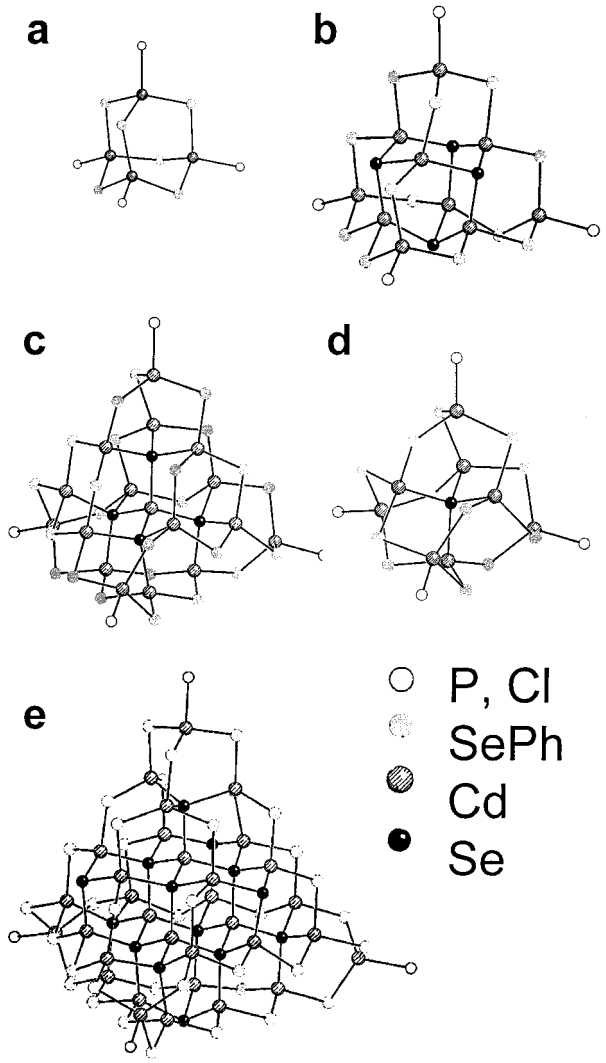

Figure 1. Structures of CdSe cluster molecules: (a) $[Cd_4(SePh)_6Cl_4]^{2-}$, (b) $[Cd_{10}Se_4(SePh)_{12}(PPr_3)_4]$, (c) $[Cd_{17}Se_4(SePh)_{24}(PPh_2Pr)_4]^{2+}$, (d) $[Cd_8Se(SePh)_{12}Cl_4]^{2-}$, and (e) $[Cd_{32}Se_{14}(SePh)_{36}(PPh_3)_4]$.

present a systematic study of the size-dependent optical and electronic properties of a homologous series of CdSe cluster molecules with 4, 8, 10, 17, and 32 Cd atoms, which represent the ultimate molecular limit of the bulk semiconductor (Figure 1).

In the larger nanocrystals, the detailed size dependence of the excited-state transitions has been studied with photoluminescence excitation (PLE) spectroscopy.[9,19,20] The inherent inhomogeneous broadening present in the absorption spectra, due mainly to the variance in nanocrystal sizes, was partially overcome by size-selective PLE, in which a narrow detection window on the blue side of the luminescence selectively probes a subset of the smaller nanocrystals in the ensemble. Up to 10 transitions were mapped and the involved electronic structure was assigned with the use of an effective mass based theoretical description,[9] or a more atomistic approach using pseudopotentials.[21] In cluster molecules, such a systematic study has not been reported yet. Clearly, size variance should be absent as a source for inhomogeneous spectral broadening but the optical transitions measured for various II−VI semiconductor cluster molecules are broad, and the source of the broadening is still unclear.

Moreover, observed optical transitions in CdS and ZnS based compounds did not manifest systematic size-dependent behavior. $Cd_{32}S_{50}$ clusters with thiophenols exhibited absorption with a first peak at 360 nm,[2] while the first absorption peak of similar clusters capped by aliphatic thiols was at 325 nm.[22] For a $Cd_{17}S_{30}$ cluster, the first absorption peak is shifted further to the blue, to 290 nm.[3] Smaller CdS cluster compounds did not exhibit a systematic blue shift with reduced size and this was assigned to the contribution of transitions related to the surface ligands.[5,6] Strong mixing with transitions related to the capping thiophenol ligands was also suggested for ZnS cluster molecules.[23] This assignment was based on electronic structure calculations, and the positions and oscillator strengths of the calculated transitions were in agreement with the measured absorption spectra. In CdSe, the bulk band gap is red shifted compared with both CdS and ZnS (1.7 eV versus 2.4 and 3.5 eV, respectively), and a larger range of energetic shift is possible prior to significant mixing of the band gap transition with the transitions of the surface ligands. This provides further motivation to investigate the size-dependent optical spectra of CdSe cluster molecules.

In the larger nanocrystals, the surface plays an important role in determining the nature of the emission.[24−28] Deep trap emission occurs in cases of imperfect passivation of the surface, which creates sub gap electronic states.[29] This emission is broad, substantially red shifted from the absorption onset, and is characterized by long lifetimes. In the cluster molecules, the role of surface atoms in the emission should be even more pronounced, and in all previous studies,[2−4] the emission exhibited characteristics that resemble those of the deep trapped emission of nanocrystals. An additional phenomenon discovered in time traces of the emission of single nanocrystals is the on−off blinking behavior of the fluorescence.[30−33] This blinking was assigned to temporary darkening of the nanocrystal due to reversible charging with an excess electron or hole trapped in the surrounding ligand shell or in the matrix. The detailed nature of this process is presently under intense investigation, and its possible relevance to cluster molecules should be considered in light of the dominance of surface atoms.

Here, we use CdSe cluster molecules as a prototypical homologous series to study the molecular limit of the bulk, and to further investigate the role of the surface ligands in their electronic properties. Particular focus is given to the nature of

(19) Banin, U.; Lee, C. J.; Guzelian, A. A.; Kadavanich, A. V.; Alivisatos, A. P.; Jaskolski, W.; Bryant, G. W.; Efros, A. L.; Rosen, M. *J. Chem. Phys.* **1998**, *109*, 2306.
(20) Bertram, D.; Micic, O. I.; Nozik, A. J. *Phys. Rev. B* **1998**, *57*, R4265.
(21) Wang, L. W.; Zunger, A. *J. Phys. Chem.* **1998**, *102*, 6449.
(22) Vossmeyer, T.; Reck, G.; Schulz, B.; Katsikas, L.; Weller, H. *J. Am. Chem. Soc.* **1995**, *117*, 12881.
(23) Bertoncello, R.; Bettinelli, M.; Casarin, M.; Maccato, C.; Pandolfo, L.; Vittadini, A. *Inorg. Chem.* **1997**, *36*, 4707.
(24) Chestnoy, N.; Harris, T. D.; Hull, R.; Brus, L. E. *J. Phys. Chem.* **1986**, *90*, 3393.
(25) Wang, Y.; Herron, N. *J. Phys. Chem.* **1988**, *92*, 4988.
(26) Bawendi, M. G.; Carroll, P. J.; Wilson, W. L.; Brus, L. E. *J. Chem. Phys.* **1992**, *96*, 946.
(27) Guzelian, A. A.; Katari, J. E. B.; Kadavanich, A. V.; Banin, U.; Hamad, K.; Juban, E.; Alivisatos, A. P.; Wolters, R. H.; Arnold, C. C.; Heath, J. R. *J. Phys. Chem.* **1996**, *100*, 7212.
(28) Kim, S. H.; Wolters, R. H.; Heath, J. R. *J. Chem. Phys.* **1996**, *105*, 7959.
(29) Woggon U. *Optical Properties of Semiconcuctor Quantum Dots*; Springer tracts in modern physics, No. 136; Springer-Verlag: Berlin, 1997; pp 159−174.
(30) Nirmal, M.; Dabbousi, B. O.; Bawendi, M. G.; Macklin, J. J.; Brus, L. E. *Nature* **1996**, *383*, 802.
(31) Efros, A. L.; Rosen, M. *Phys. Rev. Lett.* **1997**, *78*, 1110.
(32) Banin, U.; Bruchez, M.; Alivisatos, A. P.; Ha, T.; Weiss, S.; Chemla, D. S. *J. Chem. Phys.* **1999**, *110*, 1195.
(33) Kuno, M.; Fromm, D. P.; Hamann, H. F.; Gallagher, A.; Nesbitt, D. J. *J. Chem. Phys.* **2000**, *112*, 3117.

the emission. We first present the wavelength dependence of the photoluminescence (PL) and PLE for the full homologous series. This is followed by PL lifetime measurements and a study of the temperature dependence of PL and PLE to probe the nature of the emitting state and its relaxation dynamics. Particular attention is then given to the photostability of the cluster molecules. In the general discussion we will summarize the size-dependent properties and compare them with the larger CdSe nanocrystals.

Experimental Section

1. Synthesis. We investigated five cluster molecules in four compounds: $\{[NPr_4^+]_2[Cd_4(SePh)_6Cl_4]^{2-}\}$, $[Cd_{10}Se_4(SePh)_{12}(PPr_3)_4]$, $\{[Cd_{17}Se_4(SePh)_{24}(PPh_2Pr)_4]^{2+}[Cd_8Se(SePh)_{12}Cl_4]^{2-}\}$, and $[Cd_{32}Se_{14}(SePh)_{36}(PPh_3)_4]$[14] (Ph = phenyl, Pr = *n*-propyl). Standard Schlenk techniques were employed throughout the syntheses using a double manifold vacuum line with high-purity dry nitrogen. The solvents tetrahydrofuran, diethyl ether, and toluene were dried over sodium−benzophenone and distilled under nitrogen. Heptane was collected after refluxing over $LiAlH_4$. Anhydrous $CdCl_2$, PPh_3, and N^nPr_4Cl were purchased from Aldrich. P^nPr_3, $PhSeSiMe_3$, and $Se(SiMe_3)_2$ were prepared according to standard literature procedures.

Synthesis of $\{[NPr_4^+]_2[Cd_4(SePh)_6Cl_4]^{2-}\}$: First 0.21 g (1.15 mmol) of $CdCl_2$ together with 0.13 g (0.57 mmol) of N^nPr_4Cl were dissolved in 60 mL of dichloroethane. Then 0.44 mL (2.29 mmol) of $PhSeSiMe_3$ was added and the resulting clear solution stirred overnight. Addition of small amounts of diethyl ether led to the formation of colorless crystals of $\{[NPr_4^+]_2[Cd_4(SePh)_6Cl_4]^{2-}\}$ with a yield of 70%. Elemental analysis: C, 37.63; H, 4.64; N 1.44. Calculated values for $C_{64}H_{94}Cd_4Cl_4N_2Se_6O$: C, 38.97; H, 4.80; N, 1.43).

Synthesis of $[Cd_{10}Se_4(SePh)_{12}(PPr_3)_4]$: First 0.19 g (1.04 mmol) of $CdCl_2$ was dissolved in 40 mL of toluene under the addition of 0.41 mL (2.07 mmol) of P^nPr_3. Then 0.31 mL (1.35 mmol) of $PhSeSiMe_3$ was added and the resulting clear solution stirred overnight. Addition of 0.08 mL (0.36 mmol) of $Se(SiMe_3)_2$ led to the formation of a pale yellow solution from which $[Cd_{10}Se_4(SePh)_{12}(PPr_3)_4]$ could be crystallized by overlayering with heptane. Yield: 60%. Elemental analysis: C, 32.56; H, 3.81. Calculated values for $C_{108}H_{144}Cd_{10}P_4Se_{16}$: C, 32.81; H, 3.67.

Synthesis of $\{[Cd_{17}Se_4(SePh)_{24}(PPh_2Pr)_4]^{2+}[Cd_8Se(SePh)_{12}Cl_4]^{2-}\}$: First 0.29 g (1.58 mmol) of $CdCl_2$ was dissolved in 40 mL of tetrahydrofuran under the addition of 0.72 mL (3.16 mmol) of PPh_2-nPr. Then 0.52 mL (2.28 mmol) of $PhSeSiMe_3$ was added and the resulting clear solution stirred overnight. Addition of 0.07 mL (0.32 mmol) of $Se(SiMe_3)_2$ led to the formation of a clear solution from which $\{[Cd_{17}Se_4(SePh)_{24}(PPh_2Pr)_4]^{2+}[Cd_8Se(SePh)_{12}Cl_4]^{2-}\}$ could be crystallized by overlayering with heptane. Yield: 40%. Elemental analysis: C, 34.19; H, 2.82. Calculated values for $C_{300}H_{296}Cd_{25}Cl_4O_6P_4Se_{41}$: C, 34.95; H, 2.89.

Synthesis of $[Cd_{32}Se_{14}(SePh)_{36}(PPh_3)_4]$: First 0.27 g (1.47 mmol) of $CdCl_2$ was dissolved in 40 mL of acetone under the addition of 1.54 g (5.89 mmol) of PPh_3. Then 0.67 mL (2.94 mmol) of $PhSeSiMe_3$ was added and the resulting clear solution stirred overnight. Addition of 0.065 mL (0.29 mmol) of $Se(SiMe_3)_2$ at −30 °C led to the formation of a pale yellow solution. $[Cd_{32}Se_{14}(SePh)_{36}(PPh_3)_4]$ crystallizes from this solution after several days.Yield: 40%. Elemental analysis: C, 28.84; H, 2.136. Calculated values for for ($C_{288}H_{240}Cd_{32}P_4Se_{50}$: C, 30.42; H, 2.12.

2. Structure Determination. Single-crystal X-ray diffraction data were collected with the use of graphite-monochromatized Mo Kα radiation (λ = 0.71073 Å) at 200 K on a STOE IPDS (Imaging Plate Diffraction System) equipped with a SCHNEIDER rotating anode. All the structures were solved with the direct methods program SHELXS[34] of the SHELXTL PC suite of programs, and they were refined with the use of the full-matrix least-squares program SHELXL.[34] Molecular diagrams were prepared by using the program SCHAKAL 97.[35]

X-ray powder diffraction pattern (XRD) spectra were taken on a STOE STADI P diffractometer (Cu Kα radiation, Germanium monochromator, Debye−Scherrer geometry). Samples for the measurements were prepared by filling crystalline powders in 0.5 mm glass capillaries, which were then sealed under nitrogen.

$\{[NPr_4^+]_2[Cd_4(SePh)_6Cl_4]^{2-}\}$ crystal data: $C_{60}H_{86}Cd_4Cl_4N_2Se_6 \cdot C_4H_8O$, M = 1972.51, monoclinic, space group $P2_1/c$, a = 22.810(5) Å, b = 13.150(3) Å, c = 27.670(6) Å, β = 113.48(3)°, V = 7612(3) Å^3, at 200 K, Z = 4, D_c = 1.714 g cm^{-3}, μ(Mo Kα) = 4.149 mm^{-1}, $2\theta_{max}$ = 50°, 41042 reflections measured, 12462 unique reflections (R_{int} = 0.0348) and 8693 with $I > 2\sigma(I)$.

The structure was refined on F^2. All Se, Cd, Cl, N, and C atoms were refined anisotropically except the C atoms of THF that were refined isotropically. Positions for H atoms except those of THF were calculated to yield R = 0.0513, wR = 0.1372.

$[Cd_{10}Se_4(SePh)_{12}(PPr_3)_4]$ crystal data: $C_{108}H_{144}Cd_{10}P_4Se_{16}$, M = 3953.47, tetragonal, space group $I4_1/a$, $a = b$ = 25.441(4) Å, c = 20.308(4) Å, V = 13144(4) Å^3, at 200 K, Z = 4, D_c = 1.998 g cm^{-3}, μ(Mo Kα) = 6.103 mm^{-1}, $2\theta_{max}$ = 52°, 20262 reflections measured, 5818 unique reflections (R_{int} = 0,0721) and 4508 with $I > 2\sigma(I)$.

The structure was refined on F^2. All Se, Cd, and P atoms were refined anisotropically, C atoms isotropically. Positions for H atoms were calculated to yield R = 0.0528, wR = 0.1462.

$\{[Cd_{17}Se_4(SePh)_{24}(PPh_2Pr)_4]^{2+}[Cd_8Se(SePh)_{12}Cl_4]^{2-}\}$ crystal data: $C_{300}H_{304}Cd_{25}Cl_4O_6P_4Se_{41}$, M = 10319.01, cubic, space group $F23$, $a = b = c$ = 32.664(4) Å, V = 34849(7) Å^3, at 200 K, Z = 4, D_c = 1.853 g cm^{-3}, μ(Mo Kα) = 5.862 mm^{-1}, $2\theta_{max}$ = 50°, 37300 reflections measured, 5140 unique reflections (R_{int} = 0.1142) and 4168 with $I > 2\sigma(I)$.

The structure was refined on F^2. All Se, Cd, Cl, and P atoms were refined anisotropically, C atoms isotropically to yield R = 0.0476, wR = 0.1311 with an absolute structure parameter 0.427(16). Carbon atoms of the $PPh_2{}^nPr$ ligands with the phosphorus atom lying on the 3-fold axis could not be located for the whole phenyl ring in the difference Fourier map. This may be due to the twinning of the crystals. Attempts to calculate the structure in the lower symmetric orthorhombic space group $F222$ did not improve this situation.

An X-ray crystallographic file (CIF) for the above-mentioned compounds is given in the Supporting Information.

$[Cd_{32}Se_{14}(SePh)_{36}(PPh_3)_4]$ crystal data are given in ref 14.

2. Optical Characterization. Room temperature absorption spectra of cluster molecules in the form of suspension in Nujol were measured on a Perkin-Elmer Lambda 900 spectrophotometer with an integrating sphere. Low-temperature optical measurements were performed in a variable-temperature cryostat in the range of 5−200 K. The cryostat was mounted within a locally built fluorimeter setup, based on two monochromators. Emission was detected at right angles, after dispersion in the detection monochromator, using a photomultiplier (PMT). The excitation beam from a monochromatized 150 W high-pressure Xe arc lamp was mechanically chopped, split with a quartz plate, and detected by a Si photodiode for reference purposes. Both fluorescence and reference signals were processed with lock-in amplifiers. Resolution was varied from 1 to 4 nm. Emission spectra were corrected for the response of the detection system measured with a standard tungsten−halogen lamp, and were normalized to the excitation intensity. Excitation spectra were normalized for the excitation intensity of the lamp by the reference channel, after correction using the response curve of the photodiode.

Oil mull was found to be the best sample for low-temperature fluorescence measurements. A droplet of suspension was placed between two silica windows and the latter were fixed in the standard sample holder of the cryostat. The angle of incidence of the excitation beam was set at 20−40° from the normal to minimize reflection and scattering into the detection monochromator.

For time-resolved measurements the sample was excited by 5 ns pulses of the third or fourth harmonic of a Nd:YAG laser (Continuum

(34) Sheldrick, G. M. SHELXTL PC version 5.1 An Integrated System for Solving, Refining, and Displaying Crystal Structures from Diffraction Data, Bruker Analytical X-ray Systems, Karlsruhe, 2000.

(35) Keller, E. SCHAKAL 97, A Computer Program for the Graphic Representation of Molecular and Crystallographic Models, Universität Freiburg, 1997.

Table 1. Types and Number of Se Atoms in Cluster Molecules

cluster	μ_2 Se (bridging)	μ_3 Se (pyramidal)	μ_4 Se (tetrahedral)
Cd_4	6		
Cd_8	12		1
Cd_{10}	12	4	
Cd_{17}	24		4
Cd_{32}	36	4	10

Minilite) at 10 Hz repetition rate, and less than 1 mW power with a beam diameter of 3 mm. The fluorescence signal, after dispersion by the detection monochromator, was measured by a PMT and averaged with a digital oscilloscope (Tektronix DPO 3052). About 600 pulses were used for obtaining one decay curve. The system response time (fwhm) was 10 ns, measured by detecting the scattered laser light.

Solid state Raman spectra were measured by using a MicroRaman apparatus directly from the crystals. Far-infared spectra in the region 80−700 cm^{-1} were measured for a Nujol mull of cluster molecules between polyethylene windows.

Results and Discussion.

1. Synthesis and Characterization of a Homologous Series of CdSe Cluster Molecules. For this study, gram amounts of pure cluster-molecule compounds of all sizes were needed. The synthesis of the cluster molecules is difficult to control as all clusters are obtained by a similar reaction and their stoichiometry is nearly identical. The selectivity of the reaction was achieved by careful adjustment of the temperature, the solvent, and ratio and concentration of precursors. Forming a single crystal with cluster building blocks stringently screens the possible molecular structures. Only highly symmetric closed-shell cluster molecules can be obtained. The purity of samples used in the optical experiments was verified by measuring the powder X-ray diffraction pattern and comparing the peaks at small angles with the pattern calculated from the single-crystal diffraction data.

The molecular structures of the cluster compounds, as determined by single-crystal XRD, display structures of the published CdSe cluster cages $\{[NMe_4]_2[Cd_4(SePh)_6Br_4]\}$,[36] $[Cd_{10}Se_4(SePh)_{12}(PEt_3)_4]$,[15] $\{[Cd_{17}Se_4(SePh)_{24}(PPh_3)_4]^{2+}$-$[Cd_8Se(SePh)_{12}Cl_4]^{2-}\}$,[16] and $[Cd_{32}Se_{14}(SePh)_{36}(PPh_3)_4]$[14] (Ph = phenyl, Et = Ethyl), although Cd_4 is synthesized with a different counterion and Cd_{10} and $Cd_{17}Cd_8$ with different phosphine ligands to obtain improved yield and purity.

It is useful to realize in which way these compounds serve as a structural model for the solid. In the cluster molecules, all of the Cd atoms are four coordinated, mostly to Se atoms. Cd atoms near the tetrahedron apex are coordinated to phosphorus or chlorine as is seen in Figure 1. Thus, it is convenient to identify the various cluster molecules by the number of Cd atoms, and we use this notation throughout the manuscript. Various types of bonding can be identified for the Se atoms, which can be classified by the degree of coordination. There are tetrahedral μ_4-Se, pyramidal μ_3-Se, and bridging μ_2-Se atoms and the number of each kind of Se atom differs in the various cluster compounds as summarized in Table 1. The surface of the cluster molecules is mostly composed of phenyl groups bound to the bridging μ_2-Se. The Cd−Se bond lengths increase with decreasing coordination of the Se atoms, but they are close to the bulk value known for the zinc blende or wurtzite forms of CdSe.[14−16]

In bulk CdSe, both the wurtzite and zinc blende forms are known. Nanocrystals of CdSe prepared at high temperatures manifest the wurtzite structure,[17] while at low temperatures they form in zinc blende.[18] In the cluster molecules, a combination of both adamanthane and barylene cages, the building blocks of the zinc blende and the wurtzite structures, respectively, can be identified (Figure 1). The smaller clusters, Cd_4 and Cd_{10}, are composed only of adamanthane cages. The next cluster in this homologous series of purely cubic structures would be obtained by adding one more layer to the Cd_{10} cluster and should have the molecular formula $[Cd_{20}(\mu_4\text{-Se})_1(\mu_3\text{-Se})_{12}(\mu_2\text{-SePh})_{18}(\mu_1\text{-L})_4]^{4-}$, where L stands for the ligands at the apex positions.[37] Such high total charge for the cluster is difficult to stabilize and this may explain why such a compound was not obtained. The total charge of the next cluster in this hypothetical series, $[Cd_{35}(\mu_4\text{-Se})_4(\mu_3\text{-Se})_{24}(\mu_2\text{-SePh})_{24}(\mu_1\text{-L})_4]^{10-}$, is clearly too high. Instead, stable structures form with mixtures of adamanthane and barylene cages, a combination that changes the ratios of Se atoms with different coordination numbers and as a result reduces the total charge on the cluster. The core of the clusters is thus formed of Cd and Se atoms that are tetrahedrally bound to each other as in the solid state, and consists primarily of fused adamanthane cages, manifesting in this way the bulk structure.

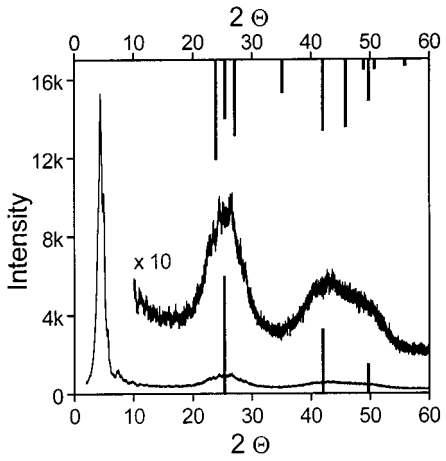

Figure 2. Powder XRD pattern for the Cd_{32} cluster molecule. Also shown are calculated spectra for hexagonal-type CdSe (upper stick spectrum) and cubic CdSe (lower stick spectrum).

The largest cluster in our series, Cd_{32}, overlaps in size with small CdSe nanocrystals prepared by Weller and co-workers.[18] Figure 2 shows the powder X-ray diffraction spectrum measured for this compound, and indeed the pattern resembles the one reported in Figure 2 of ref 18, for small CdSe nanocrystals capped by thiols. The breadth of the high-angle peaks clearly demonstrates the difficulty in characterizing the internal structure of such small clusters with powder X-ray diffraction. Transmission electron microscopy is also limited in this small size regime and, thus, one must revert to single-crystal X-ray diffraction for characterization.

2. Fluorescence Spectroscopy of CdSe Cluster Molecules. To probe the electronic structure and optical transitions of the cluster molecules, we carried out room and low temperature spectroscopic measurements. Figure 3 presents a summary of the optical data for the four compounds in the form of a suspension in Nujol. The room temperature absorption spectra are shown as short-dashed lines, and are characterized by well-defined absorption onsets, with the first transition strongly allowed.[4] The well-known phenomenon of quantum confinement that is observed for larger CdSe nanocrystals, of blue shift of

(36) Dean, P. A. W.; Vittal, J. J.; Payne, N. C. *Inorg. Chem.* **1987**, *26*, 1683.

(37) Dance, I.; Lee, G. In *Perspectives in coordination chemistry*; Lausanne, 29th International Conference on Coordination Chemistry; Williams, A. F., Ed.; Basel, Helvetica Chimica Acta; VCH: Weinheim, 1992; p 87.

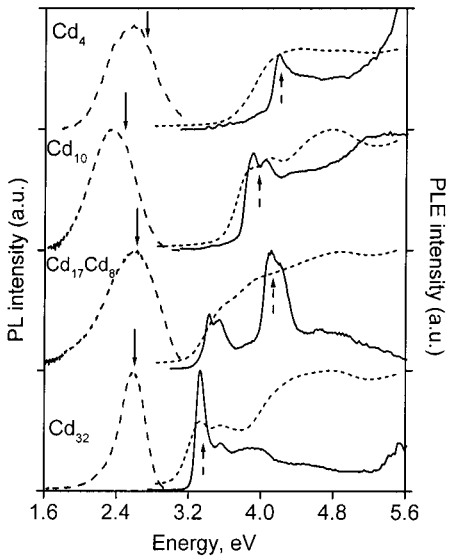

Figure 3. Summary of the spectroscopic data for CdSe cluster molecules. Absorption spectra of CdSe cluster-molecule compounds as suspensions in Nujol at room temperature are shown with dotted lines. PL spectra (dashed lines, excitation energies denoted by dashed arrows) and PLE spectra (solid lines, detection energy denoted by solid arrows) for the cluster-molecule compounds at $T = 8$ K are also shown. For clarity of presentation, the data for each compound are offset and normalized.

the absorption onset with reduced size, is sustained for the smaller cluster molecules. This systematic behavior already points out the usefulness of the CdSe clusters as a molecular model for the bulk, not only for its structure, but also for its electronic properties.

Low-temperature spectroscopic data taken at $T = 8$ K, including PL spectra (dashed lines) and PLE spectra (solid lines), are also presented in Figure 3. The PLE data display a sharp excitation onset, which shifts to the blue in the smaller cluster molecules. Compared to the room temperature absorption spectra, the PLE spectra are sharper. This is due to the substantially reduced thermal broadening at low temperature. Furthermore, the effect of scattering samples is more detrimental for the absorption measurement as compared with PLE, where our detection window is spectrally well separated from the excitation. For all cluster molecules, aside from the smallest one, several peaks are resolved. In particular, for $Cd_{17}Cd_8$, which has a structure-less absorption, two structured peaks are resolved, at approximately 3.5 and 4.1 eV. All the cluster molecules exhibited intense green-blue emission at low temperatures. The PL is broad and red-shifted substantially from the excitation onset. The PL peak position is nearly independent of the cluster size, suggesting that the origin of the emitting state is similar in all species.

More detailed information is obtained by measuring the PL and PLE spectra at different excitation and detection energies, respectively. This kind of measurement can reveal what species are responsible for the emission, and it is also useful in checking the purity of the samples. A Series of PL spectra were obtained at $T = 20$ K for each cluster molecule, at different excitation energies, starting from 4.6 eV (270 nm) going to lower energy with 10 nm steps until only the weak background signal could be detected. The series of PLE spectra was obtained in the same manner, changing the emission detection window from 1.8 eV (640 nm) up to the absorption onset with 20 nm steps. For the cluster-molecule compounds Cd_4, Cd_{10}, and Cd_{32}, which are composed of a single cluster type, the normalized

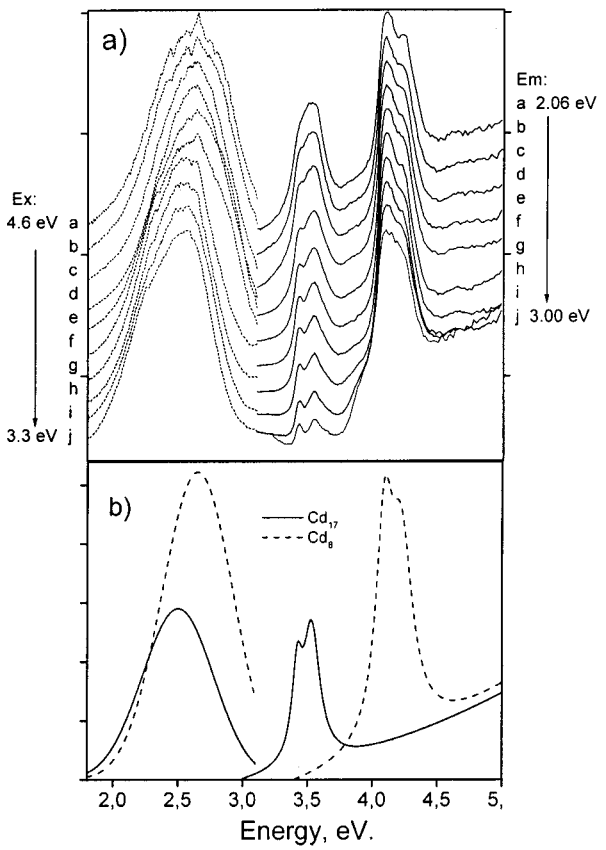

Figure 4. (a) A full series of normalized PL and PLE spectra of the Cd_8Cd_{17} cluster molecule. PLE spectra are normalized on the height of the higher energy peak. Spectra are shifted for clarity by 0.1 one from another. (b) Simulated PL and PLE spectra of Cd_{17} (dashed line) and Cd_8 (solid line) extracted from the model. See text for details.

PL and PLE spectra are nearly identical in shape (see Figure S1 in the Supporting Information). This lack of wavelength dependence provides strong evidence for the purity of the samples.

A different behavior is observed in the case of the $Cd_{17}Cd_8$ compound for which the complete wavelength dependence of PL and PLE spectra is shown in Figure 4a. The PL spectra (Figure 4a, dotted lines) are normalized on the emission maximum and are offset from each other by 0.1. The PL peak position slightly shifts to the red upon lowering the excitation energy. The PLE spectra (Figure 4a, solid lines) are normalized on the height of the high-energy peak at 4.1 eV and are also separated by 0.1. The relative height of the lower energy structured peak at 3.5 eV decreases systematically upon increasing the detection energy. At a detection energy of 2.06 eV the ratio of the high-energy peak to the low-energy peak is 1.5:1, increasing substantially to 6:1 at a detection energy of 3.0 eV. These systematic changes indicate that there is more then one emitting species in the $Cd_{17}Cd_8$ compound.

As an explanation to this wavelength dependence of the PL and PLE, we suggest that the Cd_8 and Cd_{17} clusters in the $Cd_{17}Cd_8$ compound emit almost independently in the sample, and have different absorption spectra. Consistent with the expected shift due to the quantum confinement, we assign the low-energy excitation peaks at 3.5 eV to the larger Cd_{17} cluster, and the high-energy peaks at 4.1 eV to the Cd_8. Therefore, there is a smooth transition from emission of Cd_8 to emission of Cd_{17} upon lowering the excitation energy. The PL spectra of both clusters are slightly shifted relative to each other, and may have different widths, leading to the observed dependence of the PLE

spectra on the detection energy. We also considered the possibility of energy transfer from Cd_8, the donor, to Cd_{17}, the acceptor, a mechanism supported by the photodarkening experiments presented in subsection 4.

This assignment is substantiated by simulations, in which the total PL of the sample is calculated as a linear combination of the two emission bands with coefficients proportional to the number of photons absorbed by each type of cluster molecule. Figure 4b summarizes the model showing the extracted emission and excitation spectra for the Cd_{17} and Cd_8 clusters (dashed and solid lines, respectively). We assumed a Gaussian shape for the emission spectra, and the excitation spectrum of each cluster was modeled by two closely lying Lorentzian peaks representing the absorption onset and a close-lying excited state, followed by a cubic polynome that represents absorption to higher states. The PL at different excitation energies were calculated using eq 1

$$PL(\nu_f;\nu_e) = [A_{Cd_{17}}(\nu_e) + \alpha\cdot A_{Cd_8}(\nu_e)]\cdot F_{Cd_{17}}(\nu_f) + (1-\alpha)\cdot A_{Cd_8}(\nu_e)\cdot F_{Cd_8}(\nu_f) \quad (1)$$

with $PL(\nu_f;\nu_e)$ the fluorescence at the varying frequency ν_f excited at a fixed value of ν_e calculated as a sum of the PL spectra of Cd_8 and Cd_{17} at ν_f represented by $F_{Cd_8}(\nu_f)$, and $F_{Cd_{17}}(\nu_f)$, respectively, weighted by the relative absorption at ν_e represented by $A_{Cd_8}(\nu_e)$ and $A_{Cd_{17}}(\nu_e)$, respectively. α represents the extent of energy transfer from Cd_8 to Cd_{17} and can vary in the range of 0, corresponding to no energy transfer, to 1, corresponding to complete transfer. The PLE spectra, $PLE(\nu_e;\nu_f)$ at the variable excitation frequency ν_e at a fixed detection frequency ν_f were obtained in a similar way. The parameters were varied until the complete sets of experimental PL and PLE spectra (22 curves) could be fit simultaneously (see Figure S2 in Supporting Information).[38]

The simulated spectra are nearly in quantitative agreement with the experiment. The changing ratio of the excitation peaks associated with the two clusters is well reproduced in the simulation, along with the actual intensity changes. The successful simultaneous modeling of all the PL and PLE spectra shows that the fluorescence of the $Cd_{17}Cd_8$ compound is a combination of the fluorescence of the two cluster molecules Cd_{17} and Cd_8. This verifies the purity if this compound as well, and establishes our assignment of the low-energy peaks in the excitation spectra to Cd_{17} and the high-energy peaks to Cd_8.

3. Nature of the Emitting State and Its Relaxation Dynamics. While the absorption onset displays a systematic blue shift in smaller cluster molecules, the emission peak positions are nearly identical for the entire series. Furthermore, the PL spectra are broad, considerably red shifted from the absorption onset, and no emission could be detected at room temperature. These properties resemble the characteristics of the "deep trapped emission" in larger nanocrystals, which arises from forbidden transitions of surface states. To further probe the nature of the emission we measured the fluorescence lifetimes. Figure 5 shows the measured PL decay data for the various cluster molecules at $T = 10$ K, normalized to 1 at time zero. The fluorescence decay was monitored at the emission peak maximum. For Cd_{32} and Cd_{17} the data were obtained by excitation at 355 nm, while for Cd_{10} and Cd_4 excitation at 266 nm was used. For Cd_{32}, excitation at 266 nm yielded similar decay curves. For all cluster molecules long decay times are observed as expected for an optically forbidden transition, and the decay times vary being fastest for Cd_{32} and slowest for Cd_4.

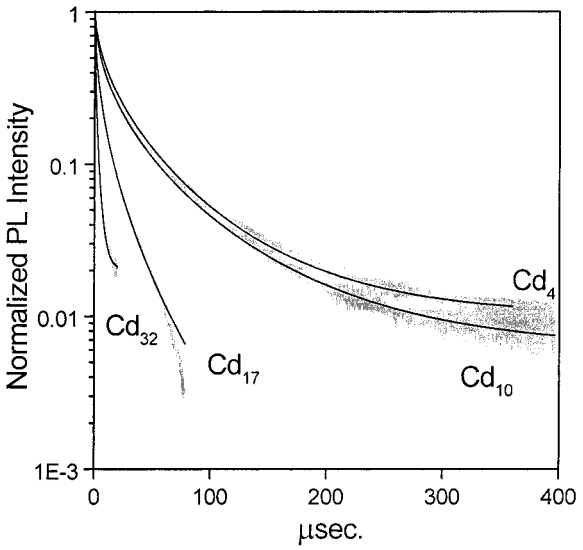

Figure 5. Normalized time-resolved PL decay traces for CdSe cluster molecules at $T = 10$ K. Solid lines show the fits to the single Williams–Watts stretched exponential function.

Table 2. Parameters of the Fits of Luminescence Decays of the CdSe Cluster Molecule to the Williams–Watts Function [$I(t) = A + \exp(-(t/\tau)^{\beta})$] (left columns) and Fit of Temperature Dependence of PL to Multiphonon-Induced Relaxation Theory (right columns)

fits of luminescence decays					fit of temperature dependence			
cluster	A	τ (μs)	β	χ^2	$\hbar\omega_m$ (cm^{-1})	G	C/k_r ($cm^{-2}s^{-1}$)	ΔE (cm^{-1})
Cd_4	0.01	10.0	0.54	1×10^{-5}	302	69	0.075	20700
Cd_{10}	0.003	9.8	0.49	6×10^{-6}	302	63	0.74	18950
Cd_{17}	0	3.1	0.50	1×10^{-5}	302	68	0.73	20400
Cd_{32}	0.019	0.78	0.59	2×10^{-5}	192	62	105	20800

The decay curves are clearly nonexponential as was observed previously for trapped emission in CdS and PbI_2 semiconductor nanocrystals.[24,25,39] We could not fit them using a sum of up to three exponential decay functions, implying the presence of distributed kinetics in the excited-state decay in the cluster molecules. For the normalized signal, the distributed kinetics is described by the Williams–Watts stretched exponential form[40]

$$I(t) = \exp[-(t/\tau)^{\beta}] \quad (2)$$

This empirical function was originally successfully used in the description of dielectric relaxation and is applicable to relaxation processes with a distribution of decay times, the width of which is reflected by β with τ a mean decay time. It was also applied to describe the decay curves of trapped emission of semiconductor nanocrystals, in which a distribution of trap sites on any given particle, as well as the distribution of particles, lead to distributed decay kinetics.[39,41] The fits are shown as solid lines in Figure 5 and the parameters are given in Table 2, which shows that τ varies from 0.8 μs for Cd_{32} up to 10 μs for Cd_4 while β is on the order of 0.5 for all cluster molecules.

(38) The following parameters (position of maximum, width of peak, extent of energy transfer) were used for the simulation of the PL and PLE of $Cd_{17}Cd_8$. $\nu_{maxPL\ Cd17} = 2.53$ eV, $W_{PL\ Cd17} = 0.55$ eV, $\nu_{maxPLE\ Cd17} = 3.42$ and 3.53 eV, $W_{PLE\ Cd17} = 0.09$ and 0.16 eV. $\nu_{maxPL\ Cd8} = 2.63$ eV, $W_{PL\ Cd8} = 0.55$ eV, $\nu_{maxPLE\ Cd8} = 4.09$ and 4.22 eV, $W_{PLE\ Cd8} = 0.15$ and 0.22 eV, $\alpha = 0.2$.

(39) Dag, I.; Lifshitz, E. *J. Phys. Chem.* **1996**, *100*, 8962.
(40) Williams G.; Watts, D. C. *Trans. Faraday Soc.* **1970**, *66*, 80.
(41) O'Neil, M.; Marohn, J.; McLendon, G *J. Phys. Chem.* **1990**, *94*, 4356.

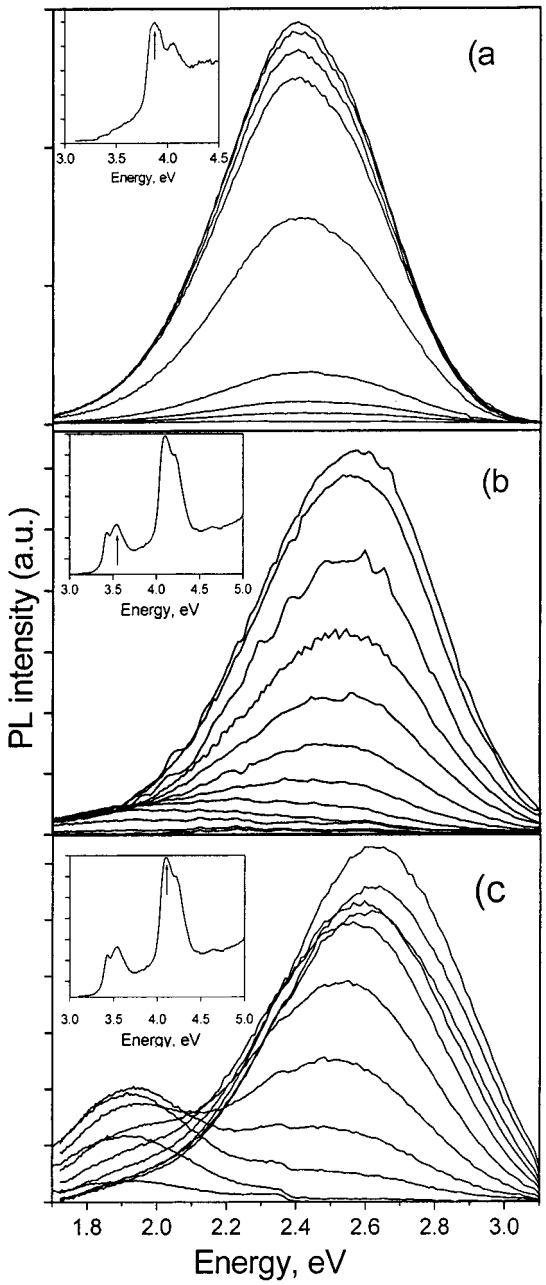

Figure 6. (a) Temperature dependence of the PL of Cd_{10} for $T = 8-120$ K. From top to bottom traces, the temperatures are 8, 20, 30, 40, 50, 60 70, 80, 100, and 120 K. (b and c) Temperature dependence of PL of the Cd_8Cd_{17} cluster molecule in the range 5−120 K exciting on the Cd_{17} peak maximum (b) and the Cd_8 peak maximum (c). From top to bottom traces, the temperatures are 5, 10, 20, 30, 40, 50, 60, 70, 80, 100, and 120 K. Insets show the positions of the excitation energies on a representative PLE spectra for each case.

The decay time τ is related to both the radiative (k_r) and nonradiative (k_{nr}) decay constants through $1/\tau = k_r + k_{nr}$. To estimate k_r we also estimated the QY of the cluster molecules, by comparing the emission intensity for a completely absorbing sample at low temperatures with the emission intensity of a fully absorbing solution of R6G dye in methanol at room temperature.[42] The QY of the brightest cluster molecule, Cd_{17}, within compound $Cd_{17}Cd_8$ was estimated to be ~40% at $T = 10$ K. By relative comparison of the emission intensity of the other cluster molecules with that of Cd_{17}, we estimate that the low-temperature QY ranges from 10 to 30% for the various cluster molecules.

To determine the mode of nonradiative relaxation from the emitting state, we studied the dependence of the PL intensity on temperature. For each cluster-molecule compound, the emission, excited on the first PLE maximum, was measured at various temperatures starting from $T = 5$ K, and up to 150−200 K where the PL intensity was reduced to the background level. To minimize the effect of photodegradation during these experiments, low excitation intensities were used, and after measuring the PL at the highest temperature, the sample was cooled back to the base temperature and the PL and PLE at this temperature were measured again. The differences between the spectra at the beginning of the cycle and at the end were less than ~20%.

Figure 6a shows the series of PL spectra at different temperatures for Cd_{10}, and the inset shows a representative PLE spectrum with the position of the excitation indicated by an arrow. The PL decreases with increasing temperature, and a similar behavior was observed for Cd_4 and Cd_{32} (see Figure S3 in Supporting Information). A somewhat different behavior for the temperature dependence of the PL was found for $Cd_{17}Cd_8$, which is presented in Figure 6b,c. In this case, at each temperature, the PL was measured with two different excitation energies for Cd_{17} and Cd_8 as assigned in the previous section. Figure 6b shows the dependence upon excitation at 3.6 eV, for the Cd_{17} cluster molecule, while the dependence for Cd_8 is shown in Figure 6c with excitation at 4.1 eV. Here, in addition to the general decrease in the PL intensity accompanied by the red shift with increasing temperature, a new emission band appears at lower energy. This is most pronounced for the Cd_8, which displays a new emission peak at 1.9 eV indicating a temperature-activated relaxation into a lower lying state.

The general temperature dependence of the PL can be comprehended within the framework of emission related to forbidden surface states. At room temperature, the fast nonradiative decay processes efficiently compete with the long radiative recombination from these states, and as a result no emission can be observed. Upon cooling, the nonradiative rates decrease substantially, and the emission quantum yield increases. A common method, useful in the assignment of the nonradiative relaxation dynamics, is to plot the ratio between the integrated PL intensity at the base temperature, I_0, and the integrated PL intensity at higher temperatures, I_T. These data are presented in Figure 7 for all the cluster molecules aside from Cd_8, which shows a more complex behavior as discussed above.

The ratio I_0/I_T is related to the radiative rate k_r and the nonraditive rate k_{nr} by

$$I_0/I_T = (1 + k_{nr}/k_r)/(1 + k^o_{nr}/k_r) \qquad (3)$$

With k^o_{nr} the value of the nonradiative rate constant at the lowest temperature. We first tried to fit the experimental dependence assuming an Arrhenius form for k_{nr}. One important common feature observed for all the cluster molecules is that the emission intensity stays nearly unchanged from $T = 5$ K up to 50 K, while further heating quickly quenches the luminescence. This nonexponential temperature dependence of I_0/I_T could not be reproduced with the Arrhenius model. Instead, we employed a different theory, of mutiphonon induced nonradiative relaxation, for the temperature dependence of k_{nr}. Different theoretical variants of multiphonon relaxation[43,44] have been applied to explain the temperature dependence of surface-trapped emission

(42) The emission from the dye solution was measured in the cryostat at room temperature under the same conditions (excitation, geometry, and detection) as those used for the cluster molecules. We used front face excitation of a fully absorbing sample in a home-built cell with an optical path length of 0.5 mm.

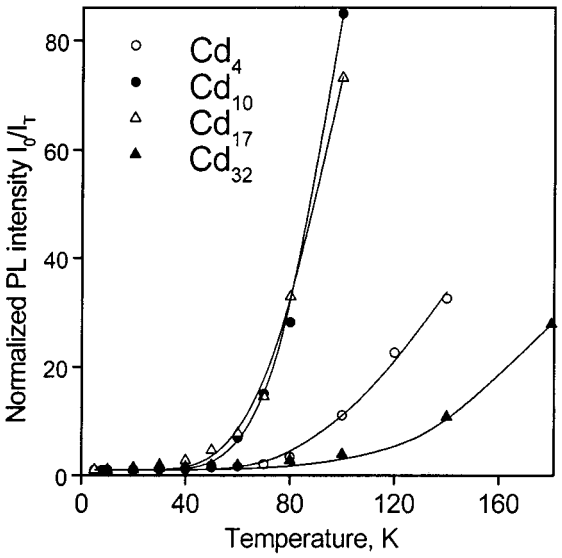

Figure 7. Summary of the temperature dependence of the PL intensity of CdSe cluster molecules. Shown is the ratio of the integrated PL at the base temperature $T_0 = 5$ K (I_0) to the integrated PL at higher temperatures (I_T). The experimental points are presented by the symbols with the cluster size designated in the legend. Fits to the multiphonon radiationless relaxation theory (see text) are presented with solid lines.

of CdS and PbI2 nanoparticles.[24,25,39] We used the version developed by F. Fong, which was originally used to explain the temperature dependence of emission of rare-earth ions in solids.[43]

In this treatment, the nonradiative relaxation takes place via coupling of the excited state to a lower lying electronic state displaced along a dominant mediating phonon mode with frequency ω_m. The relaxation rate depends on the energy detuning between the lowest lying vibrational level of the upper electronic state and high vibrational levels of the lower electronic state assumed to be harmonic, and on the Franck−Condon displacement between the two states as detailed for example in ref 25. The similar nature of the emission and its temperature dependence in all the cluster molecules prompted us to look for a common mediating frequency, ω_m, present in all the compounds. To determine the possible mediating frequencies in the multiphonon relaxation process, we have measured the solid-state vibrational spectra of the cluster molecules using far-infrared and Raman spectroscopy (see Figure S4 in the Supporting Information). Several common vibrational modes were observed, and in particular one with a frequency of 302 cm^{-1}, which is both IR and Raman active. Using this single mediating frequency we succeeded in fitting the temperature dependence of I_0/I_T of three compounds, Cd_4, Cd_{10}, and Cd_{17}, while a different mediating frequency, 192 cm^{-1}, was found for Cd_{32}. The fits are shown as the solid lines in Figure 7, and were obtained by using the energy separations ΔE between the emitting state and the ground state, taken as the maximum of the PL peak. There are two free parameters: the Franck−Condon displacement, G, and the factor C/k_r, where C is the electronic coupling strength and k_r is the radiative rate constant. All the parameters are given in Table 2.

A particularly noteworthy result is that for three cluster molecules (Cd_4, Cd_{10}, Cd_{17}), the same value for the mediating frequency, $\omega_m = 302$ cm^{-1}, was found. This frequency was also observed in the far-IR spectra of Se_2Ph_2 molecules, and is most likely assigned to bending vibration of the selenophenol group. In S_2Ph_2 molecules this band shifts to higher frequency (most probably to 400 cm^{-1}), consistent with the involvement of the M−Ph group in this vibrational mode. This indicates that the nonradiative relaxation is mediated via a vibrational mode of the surface selenophenol ligands, consistent with the assignment of the emitting state to forbidden transitions related to the cluster surface ligands. Various such transitions are possible because of the different surface sites on any given cluster. An additional source for a distribution of such sites is the different environments possible for differently packed clusters within the microcrystalline powder. This is consistent with the observation of the distributed decay kinetics through the lifetime measurements.

In the larger Cd_{32} cluster, the lower mediating frequency (192 cm^{-1}) is at the center of a broad strong peak detected in both the IR and Raman spectra. This frequency is close to the bulk longitudinal optical (LO) phonon mode of CdSe at 210 cm^{-1},[45] and may therefore involve the stretching vibrations of interior Cd−Se bonds. Another possibility for the assignment of this frequency is to the Cd−Se−Ph vibrational mode. This latter assignment gains support from previous work on IR spectra of CdS cluster molecules.[46] Compared with the smaller cluster molecules, for Cd_{32}, interior modes are therefore more strongly involved in the nonradiative relaxation from the emitting state. This is consistent with the higher density of interior vibrational states in Cd_{32}, and with the analysis of the relaxation dynamics in larger free-standing CdS nanocrystals.[24]

4. Photodarkening of Cluster Molecules. In our experiments we observed a decrease of the emission intensity after illumination of the cluster molecules at low temperature with the Xe lamp. We investigated this photodarkening effect systematically by irradiating the cluster molecules at 300 nm and under similar irradiation conditions (for Cd_{17} 350 nm was used), and we followed the decay of the intensity at the PL maximum versus irradiation time. The irradiation intensity was on the order of 10 μW with a spot diameter of ~3 mm. We found that the degradation time is size dependent with Cd_{32} the fastest (time scale of ~5 min) and Cd_4 the slowest (time scale of over an hour), and this is related to the amount of excess energy of excitation relative to the absorption band gap. The excess energy is the largest for Cd_{32} leading to the fastest decay, while when irradiating the same sample at 360 nm, close to the gap of Cd_{32}, only very slow degradation (time scale of hours) is observed.

The effect of irradiation on the emission and excitation spectra is shown in Figure 8 for Cd_4, Cd_{10}, and Cd_{32} (frames a, b, and c, respectively). The solid lines represent the initial emission and excitation spectra at low temperature, while the dashed−dotted lines correspond to spectra detected following irradiation. For Cd_{10} several intermediate spectra are shown, and the first minutes of the irradiation lead to significant narrowing of the excitation spectra. For Cd_{32} a narrowing of the PLE is also observed upon irradiation as can be seen clearly in the inset of frame c, which shows normalized PLE spectra before (solid line) and after (dash−dotted line) irradiation.

To test if the photodarkening is permanent, we heated the samples up to $T = 200$ K for 20 min in the dark, and then re-cooled them. The spectra after this heating−cooling cycle are shown in Figure 8 as the dotted lines. Interestingly, the

(43) Fong, F. K.; Wassam, W. A. *J. Chem. Phys.* **1973**, *58*, 956.
(44) Jortner, J. *J. Chem. Phys.* **1976**, *64*, 4860.
(45) Madelung, O.; Schulz, M.; Heiss, H., Eds. *Landolt-Bornstein: Numerical Data and Functional Relationships in Science and Technology*, New Series; Springer-Verlag: New York, 1982; Vol. 17.
(46) Lover, T.; Bowmaker, G. A.; Seakins, J. M.; Cooney, R. P. *Chem. Mater.* **1997**, *9*, 967.

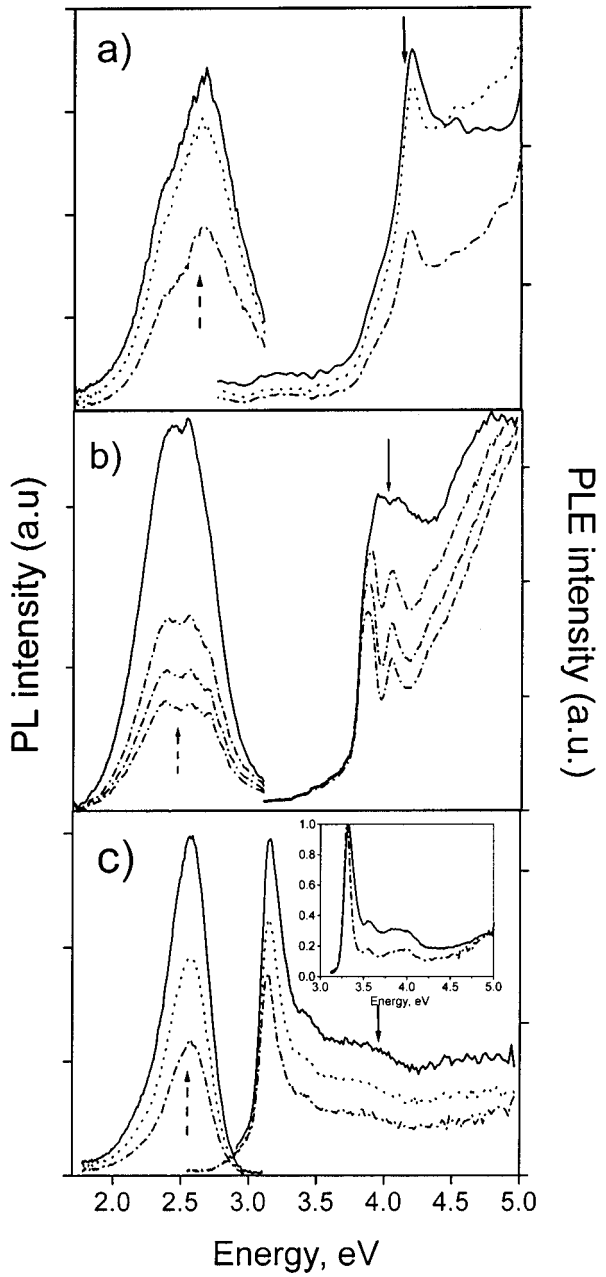

Figure 8. Photodegradation of CdSe cluster molecules. The irradiation energies are indicated by solid arrows. Shown are PL and PLE (detection energies indicated by dashed arrows on the PL) spectra. Solid lines represent the initial spectra at low temperature. Dash−dotted lines represent the spectra after irradiation for 110 min for Cd_4 and 5 min for Cd_{32} cluster molecules at $T = 20$ K. For Cd_{10} (frame b) several intermediate spectra are shown, after 25, 65, and 120 min of irradiation, and the narrowing of the PLE upon irradiation is clearly observed. Narrowing of the first excitation peak is also observed for Cd_{32} as shown in the inset of frame c, which presents normalized PLE spectra of the initial (solid line) and irradiated (dash−dotted line) sample. For Cd_4 (frame a) and Cd_{32} (frame c), recovered low-temperature spectra after a warm-up−cool-down cycle are shown with dotted lines.

emission of Cd_4 nearly fully recovers, and the emission of Cd_{32} partially recovers. Cd_{10} emission did not recover and is therefore not shown.

The partially reversible photodarkening indicates that this process is not primarily related to photochemical degradation of the cluster molecules. We also measured the transmission spectrum of Cd_{32} and Cd_{10} before and after irradiation at low temperature and the transmission of the scattering samples was nearly unchanged, consistent with the absence of substantial photochemical reactions altering the cluster interior. The nonreversible degradation processes that may take place are therefore modifications of the cluster-molecule surface, such as photochemical cleavage of the Se−Ph bonds, which would affect the emission, and this may explain the nonreversible photodarkening. These kinds of processes may also explain the narrowing of the PLE spectra of Cd_{10} upon irradiation. The clusters with incomplete surface coverage will quickly degrade and become dark, thus reducing the width of the inhomogeneous distribution of the emitting clusters. Therefore an important inhomogeneous broadening mechanism in cluster molecules of a single size is the surface "quality".

In contrast with the above mechanism, the reversible portion of the PL can be associated with temporary charging of the cluster molecules, with the counter-charge trapped either in the Nujol environment or on the ligand shell. Such charging should not completely alter the absorption but will quench the emission via efficient nonradiative Auger recombination of the electron−hole pair induced by the excess charge.[30,31] This charging requires sufficient energy for the ionization of the cluster molecule. This may take place either by a sequential two-photon process, in which the first photon creates a long-lived excited state that is then ionized by a second photon, or by single photon excitation followed by trapping of one charge carrier in the surrounding of the cluster core. By raising the temperature, the cluster is neutralized via recombination of the excess charge, which is a thermally activated process. A similar photodarkening process was previously reported for CdS nanocrystals in glass, where an increase of the darkening efficiency was observed when irradiating the sample with light above the barrier for transitions of electrons from the nanocrystals to the glass.[47] The temporary darkening mechanism may also be closely related to the analogous "blinking" phenomena of the photoluminescence detected for single CdSe nanocrystals.[30−33] The surface of the nanocrystals most probably provides the trap sites for excess charge. In the cluster molecules where most of the atoms are surface atoms, the darkening phenomena should be significant as we indeed observe.

More involved behavior was observed in the photodarkening of the $Cd_{17}Cd_8$ compound as summarized in Figure 9. Frame a shows the initial PLE spectrum at low temperature in solid line. The dash−dotted line presents the PLE spectrum following extensive irradiation at 350 nm, on the excitation peak assigned to Cd_{17}. Quenching by a factor of 3 of the excitation peak at 3.5 eV is seen, accompanied by a decrease in the intensity of the peak at 4.1 eV by $\sim 1/3$, after subtracting the decrease related to the excited-state absorption of Cd_{17}. Quantitative restoration of both peaks in the PLE spectrum was observed after heating the sample to $T = 200$ K, and re-cooling (dotted line). This same spectrum is shown as a solid line in frame b, which presents the continuation of this experiment. The irradiation wavelength was set to 300 nm, on the excitation peak assigned to Cd_8. After the irradiation, nearly complete quenching (by a factor of 6) of the PLE peak at 4.1 eV was seen (dash−dotted line). The extensive irradiation also led to some quenching of the peak at 3.5 eV (by a factor of 2). After an additional warm-up−cool-down cycle, the PLE was nearly restored to its original intensity (dotted line).

The photodarkening of the low-energy peak after irradiation at 4.1 eV (Figure 9b) can be comprehended taking into account the absorption of Cd_{17} to higher excited states, which were considered in our model of the wavelength dependence of the

(47) Ekimov, A. I.; Efros, A. L. *Phys. Status Solidi B* **1988**, *150*, 627.

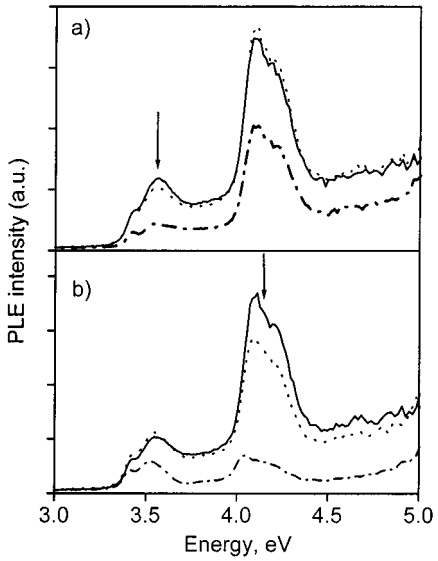

Figure 9. Influence of iradiation and warm-up−cool-down cycling on the PLE spectra of the $Cd_{17}Cd_8$ cluster molecule: (a) irradiating for 40 min at the Cd_{17} peak maximum and (b) irradiating for 20 min at the Cd_8 peak maximum, as indicated by the arrows. Solid lines represent the initial spectra at $T = 20$ K. Dash−dotted lines represent the spectra after irradiation at low temperature. Recovered low-temperature spectra after a warm-up−cool-down cycle are shown with dotted lines.

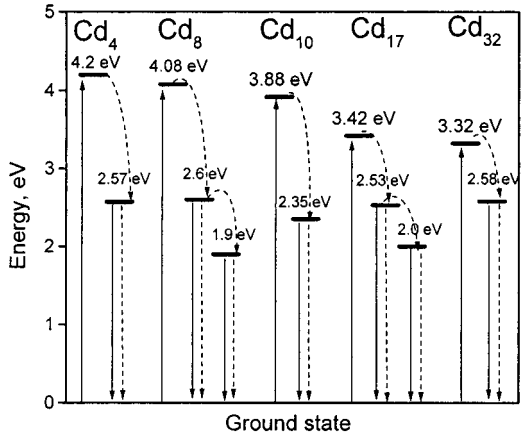

Figure 10. Summary of the electronic levels for all studied CdSe cluster molecules. See text for details.

PL and PLE shown in Figure 4. The degradation of the high-energy peak in the PLE spectrum taken after the lower energy irradiation (Figure 9a) can be explained by energy transfer between Cd_8, the donor, to Cd_{17}, the acceptor, also included in the above-mentioned model. As Cd_{17} is photodarkened, the fraction of the excitation intensity of Cd_8, which is related to the energy transfer to the acceptor, is also quenched. In our modeling of the wavelength dependence of the PL and PLE for $Cd_{17}Cd_8$ (Figure 4), energy transfer was included and the best fit to experimental data was obtained for $\alpha = 0.2$. The assignment of the high-energy peaks to direct excitation to Cd_8 rather than to Cd_{17} is supported by the second part of the photodarkening experiment, which shows independent behavior for the quenching of the low- and high-energy excitation peaks.

General Discussion

Figure 10 summarizes the spectroscopic data for the positions of states for the homologous series of cluster molecules. The absorption onset systematically blue-shifts in smaller cluster molecules, reaching a value of 4.2 eV for the Cd_4 cluster. The systematic shift of the absorption onset signifies that even in these small molecular compounds, the size of the cluster plays a dominant role in determining the band gap, and the "interior" states may be probed independently from the "surface" states. The concepts of quantum confinement, widely applicable to the larger nanocrystals, are still useful for understanding the behavior of the molecular cluster compounds.

On the other hand, the emitting state in all cluster molecules lies at a similar energy and does not show systematic size dependence. It is substantially red-shifted from the absorption onset of all compounds. The emission transition is forbidden, as is clear from the long lifetimes (microsecond time scale), and from the complete quenching of the fluorescence above $T = 150-200$ K. We therefore assigned this transition to emission from "surface" states. More specifically, the analysis of the temperature dependence of the emission points to a possible trap state on the bridging selenophenol ligands and this assignment presents a theoretical challenge for quantum-chemical methods for electronic structure calculations.[48]

It is noteworthy that even in such small molecules, the "surface" plays a distinct role. Surface effects known from the larger nanocrystals are enhanced by the dominance of surface atoms, for example, only "trapped emission" was detected for the cluster molecules. We also observe temporary photdarkening, which is analogous to the blinking phenomena observed for single nanocrystals. The "surface" is also a possible source of inhomogeneous spectral broadening in these compounds, and the sharpening of the PLE spectra upon irradiation directly demonstrates this effect. The possibility of inhomogeneous distribution of surface coverages by phenyl ligands may explain the broad line widths detected for such single size molecular compounds. Further support for this assignment is obtained from the study of the dependence of PL decays with emission wavelength. For all compounds, we observed increasing decay times upon shifting the PL detection position to the red, indicating the presence of several surface transitions. Single formula cluster molecules have a large number of conformational isomers, related by the pyramidal stereochemistry at each of the bridging selenophenol ligands as discussed in detail by Dance.[37] Such different conformational isomers may also affect the optical properties, specifically the PL, providing a mechanism for inhomogeneous spectral broadening.

In this work, we probed cluster molecules within their microcrystalline powders. We specifically chose this sample form because of its purity. In solution there are possibilities of dissociation of cluster molecules, and of a dynamic equilibrium between cluster molecules with different sizes. This is in fact used in the synthesis of Cd_{32}, which is prepared with Cd_{10} clusters as nucleation centers. Preliminary optical measurements of cluster molecules in solution show that the absorption spectrum has a tail to the red compared with the solid-state absorption spectra. This can be assigned to larger cluster molecules, which form in solution. In the solid-state form there is a possibility for collective interactions between neighboring cluster molecules such as electronic level mixing that can lead to "mini-band" formation.[49] The interaction should lead to a broadening of the excitation peaks in the solid-state sample, and a red shift of the excitation onset compared with dilute samples. Opposite behavior is detected when comparing the data for cluster molecules in the solid state with the spectra of dilute frozen solutions. Low-temperature optical experiments on frozen

(48) Eichkorn, K.; Ahlrichs, R. *Chem. Phys. Lett.* **1998**, *288*, 235.
(49) Capasso, F.; Faist, J.; Sirtori, C. *J. Math. Phys.* **1996**, *37*, 4775.

solutions of cluster molecules with low concentration ($\sim 10^{-5}$ M) show a broader excitation peak with energy similar to that detected in the solid state, along with a tail to the red of this peak. This indicates that the level-mixing between nearest neighbors in the super-crystal is weak. This is consistent with the high energetic barriers at the cluster surface induced by the phenyl ligands, and with the relatively large distance between clusters within the microcrystals. Therefore, the super-crystals of cluster molecules resemble a typical van der Waals bonded molecular crystal.[50]

A similar situation exists in ordered three-dimensional superlattices of larger nanocrystals.[51] The large distances and high barriers at the nanocrystal surface minimize the mixing of energy levels between neighboring particles and this phenomena could not be detected, but in this case, resonant energy transfer among the nanocrystals was observed.[52] We have also found evidence for energy transfer in the case of the mixed compound $Cd_{17}Cd_8$. This result needs to be considered within the framework of Forster-type resonant energy transfer, which requires overlap between the donor emission and acceptor absorption spectra. For the cluster molecules, the emission from the surface traps is considerably off-resonance with the absorption (Figure 3) and as a result the energy transfer from these states is less likely. On the other hand, Forster transfer may take place via the dipolar coupling of states near the absorption onset of the Cd_8 to overlapping absorbing states of Cd_{17}.

Summary

A comprehensive optical spectroscopy study of a homologous series of CdSe cluster molecules has been carried out. The absorption and low-temperature PLE onset of the clusters shifts systematically to the blue in smaller clusters, manifesting the quantum confinement effect well-known for larger CdSe nanocrystals. The emission in all cluster molecules is observed only at low temperature and is red-shifted significantly from the absorption onset. We assign the emission to optically forbidden transitions involving surface ligands, and the lifetimes are indeed in the microsecond range. The temperature dependence of the emission, which decreases significantly above $\sim T = 50$ K, was assigned to the involvement of a multiphonon nonradiative relaxation mechanism mediated by a vibration of the selenophenol surface ligands. This provides further evidence for the nature of the emitting state being involved with surface ligands. The distribution of surface states also provides a mechanism for inhomogeneous spectral broadening in single-sized cluster molecules. A photodarkening effect was detected for the cluster molecules at low temperatures. For all clusters aside from Cd_{10}, partial recovery of the emission was detected after warm-up and re-cooling. This temporary photodarkening resembles the on−off blinking behavior of the larger nanocrystals, and we assign it to photoinduced charging of the cluster molecules. Cluster molecules can be identified as the ultimate molecular limit for the bulk semiconductor.

Acknowledgment. This work was supported by the German-Israel Fund. U.B. acknowledges support of an Allon fellowship. The Farkas Research Center is supported by the Minerva Gesellschaft für die Forschung, GmbH, München. We are grateful to Fr. E. Tröster for her invaluable assistance in the synthesis of the cluster molecules.

Supporting Information Available: Tables of crystal data, structure solution and refinement, atomic coordinates, bond lengths and angles, and anisotropic parameters for Cd_4, Cd_{10}, and $Cd_{17}Cd_8$; description and figures of the wavelength dependence of PL and PLE for Cd_4, Cd_{10}, and Cd_{32}; comparison of experimental and simulated wavelength dependence of PL and PLE spectra of $Cd_{17}Cd_8$; temperature dependence of the PL for Cd_4 and Cd_{32}; and far-infrared and Raman spectra for all cluster molecules (PDF). X-ray crystallographic file for Cd_4, Cd_{10}, and $Cd_{17}Cd_8$ (CIF). This material is available free of charge via the Internet at http://pubs.acs.org.

JA003598J

(50) Pope, M.; Swenberg, C. E. *Electronic processes in organic crystals*; Oxford University Press: New York, 1982.

(51) Murray, C. B.; Kagan, C. R.; Bawendi, M. G. *Science* **1995**, *270*, 1335.

(52) Kagan, C. R.; Murray, C. B.; Nirmal, M.; Bawendi, M. G. *Phys. Rev. Lett.* **1996**, *76*, 1517. Kagan, C. R.; Murray, C. B.; Bawendi, M. G. *Phys. Rev. B* **1996**, *54*, 8633.